Published in final edited form as:
Rom J Biophys. 2013 ; 23(1-2): 81–92.

EYE MOVEMENT RECORDING AND NONLINEAR DYNAMICS ANALYSIS – THE CASE OF SACCADES[#]

Corina Aştefănoaei[*], **Elena Pretegiani**[***], **L.M. Optican**[**], **Dorina Creangă**[*], and **Alessandra Rufa**[***]

Corina Aştefănoaei: corina_astefanoaei@yahoo.com

[*]Laboratory of Biophysics & Medical Physics, Faculty of Physics, "Alexandru Ioan Cuza" University, 11, Carol I Blvd., 700506, Iași, Romania

[**]Laboratory of Sensorimotor Research, National Eye Institute, Bethesda, MD, 20892, USA

[***]Eye-tracking & Visual Application Lab EVALab, Department of Medicine Surgery and Neuroscience, University of Siena, Siena 53100, Italy

Abstract

Evidence of a chaotic behavioral trend in eye movement dynamics was examined in the case of a saccadic temporal series collected from a healthy human subject. Saccades are highvelocity eye movements of very short duration, their recording being relatively accessible, so that the resulting data series could be studied computationally for understanding the neural processing in a motor system. The aim of this study was to assess the complexity degree in the eye movement dynamics. To do this we analyzed the saccadic temporal series recorded with an infrared camera eye tracker from a healthy human subject in a special experimental arrangement which provides continuous records of eye position, both saccades (eye shifting movements) and fixations (focusing over regions of interest, with rapid, small fluctuations). The semi-quantitative approach used in this paper in studying the eye functioning from the viewpoint of non-linear dynamics was accomplished by some computational tests (power spectrum, portrait in the state space and its fractal dimension, Hurst exponent and largest Lyapunov exponent) derived from chaos theory. A high complexity dynamical trend was found. Lyapunov largest exponent test suggested bi-stability of cellular membrane resting potential during saccadic experiment.

Keywords

saccade; eye movement control; complex dynamics

INTRODUCTION

Most of the computational studies on biosignals extracted from excitable tissues and organs have been dedicated to the interpretation of electroencephalogram or electrocardiogram data recorded from normal subjects and patients with various disorders [3, 7, 8, 9, 10]. In the last years, there has been an increasing interest in using the nonlinear dynamics techniques to

[#]Presented at The 12th National Conference on Biophysics, Iaşi, June 13–16, 2013.

model oculomotor control and to analyze eye movement time series [12, 13, 14]. The study of eye movements is an important source of information on the visual-motor system, first because the presence of abnormal eye movements in a patient may help us understand how the brain works.

Some researchers focused on the eye movements recorded during reading of normal and pathological subjects, searching for evidence of chaotic, nonlinear dynamical behavior [12]. Both power spectral density analysis and fractal dimension determination showed evidence of nonlinearity as manifest for chaotic behavior. They concluded that the computed fractal dimension seemed directly related to qualitative assessment of reading ability. Analysis of another type of movement, smooth pursuit of moving targets, gave similar results.

Another study showed that optokinetic nystagmus appears to have some nonlinear and deterministic components, along with significant randomness [14]. To indicate the possibility of chaotic dynamics in such cases, the correlation dimension of these reflexive eye movements was computed, resulting in a noninteger value, signifying a fractal dimension [13].

Saccadic eye movements can be defined as rapid eye movements that shift a peripheral visual image onto the center of the retina, where it can best be seen. These rapid eye movements are designed to move the eyes as quickly as possible to minimize interference with vision [6]. Saccades can be better understood as the result of the complex integration of both motor and sensory systems. The visual system processes information coming from retinal pathways that go to the superior colliculus and visual cortices (e.g., V1 and parietal and frontal eye fields). Saccades are initiated by activity in neurons of the frontal and parietal eye fields of the cerebral cortex. These signals then follow two pathways projecting to the nucleus reticularis tegmenti pontis of the pontine reticular formation and the superior colliculus.

In this paper, we present the results of the computational approach carried out for a time series extracted during saccadic eye movements, based on chaotic determinism theory, in accord with the analysis procedure proposed by Sprott [15] in order to assess the dynamical dominant trend – quasi-periodic, chaotic or random.

MATERIAL AND METHODS

SUBJECTS

One healthy, adult male volunteer took part in eye movement research at the Laboratory of Sensorimotor Research, National Eye Institute, National Institutes of Health, USA. The subject performed a visually-guided saccade task approved by the Institutional Review Board and which conformed to the Helsinki guidelines.

APPARATUS AND EYE MOVEMENT RECORDING

The subject executed horizontal saccades in response to two red spots (3 mm diameter) acting as visual stimuli – a central fixation point and a target that could be shifted either to the left side or to the right side of the fixation point; both red light spots were projected from lasers onto a screen placed frontally at 105 cm from the subject's eye. Angular eye movements were recorded from the right eye using an infrared iView X Hi-Speed camera (SMI) eye tracking system (sampling frequency of 1,000/s). The subject response to the visual stimulation was recorded in dim light conditions. The brightness (Konica Minolta LS-110) of the fixation point and the target was 46.35 cd/m^2 and that of the background was of 0.009 cd/m^2.

EXPERIMENTAL DESIGN

In the experiment, a central spot appeared, acting as the fixation point for the subject. After a short time another spot (target) was turned on at an eccentric location (4, 6, 8, 10 or 12 degrees, leftward or rightward of fixation point). Onset of the target could follow offset of the fixation point after a short time, or it could appear synchronously with the offset of the fixation point, or it could precede the offset of the fixation point. This stimulus onset asynchrony was randomly chosen from 0, 50, 100, 150, 200, 350, or 500 ms.

The subject was asked to look at the central point until the target appeared, and then to immediately execute a voluntary saccade to the target. After the disappearance of the target, subject returned to the central point. The eye movement recording session took about 25 minutes.

The sequence chosen for the computational study had 10,000 data points – representing a median segment of the recorded signal, when the subject was familiar with the visual task but not too tired.

THEORETICAL BACKGROUND

Computational insight into the neural system coordinating eye movements was accomplished using saccadic data processing and interpretation according to the strategy proposed by Sprott and Rowlands [15] described below. This was designed based on graphical and numerical linear as well as nonlinear tests, the latest being developed according to chaos theory, especially for complex system investigation, where writing differential equations is too difficult, considering the numerous state parameters, and very difficult to identify. So, the analysis of data appearance probability, of the data power spectrum, the semiquantitative description of the so-called portrait in the state space, the evaluation of the system sensitivity to initial conditions, and other computational techniques could enable the researcher to gather the basic information for assessing the predictability in the system dynamics.

The probability distribution test provides the distribution histogram of data for any kind of signal. Periodic data from more linear processes should give a simple histogram with sharp edges; a Maxwellian distribution usually results for random data (high noise level) but this can also be the case for some so-called chaotic data extracted from very complex systems, such as biological ones; some chaotic systems are characterized by a probability distribution shape that suggests repetitive symmetry – as in the case of fractal objects.

The fast Fourier transform test involves a spectral decomposition of the recorded biosignal that displays the power (mean square amplitude) as a function of frequency (the Nyquist critical frequency, i.e. the reciprocal of twice the interval between the data points). On a log-linear scale, periodic and quasi-periodic data will provide a few dominant peaks in the spectrum. The chaotic and random data series give rise to a broad spectrum; in the chaotic series the amplitude decreases rapidly as frequency increases.

The state space test is based on interpretation of the shape of the system attractor [16] – i.e. the totality of possible equilibrium points toward which the system is attracted when it evolves with respect to the same laws but starts every time from slightly different initial conditions. It is an abstract space, often with more than three dimensions, in which the system state variables are the n position coordinates (x_1, x_2, x_3, …, x_i, x_{i+1},…, x_n) and n velocity coordinates (x_1', x_2', x_3', …, x_i', x_{i+1}',…, x_n'). The state space may be re-constructed from a single measurable variable based on its temporal variation *X(t)* together with its derivative, *X'(t)*.

In the state-space, a periodic system portrait appears as a closed loop, while a quasi-periodic system has torus like attractor; for more complex dynamics, strange attractors appear as more complicated objects, yet with a discernible shape that can be characterized by a non-integer dimension, unlike the real geometrical objects having integer Euclidian dimension from 0 to 3.

The correlation dimension test involves the calculation and interpretation of the fractal dimension of a virtual object equivalent to the system attractor. According to Schmeisser *et al*. [12], the correlation dimension is one member of an infinite family of fractal dimensions (generally non-integer), and any one of which might be used to characterize an attractor. The correlation dimension (*CD*) can be calculated [4] from the correlation integral $C(r)$:

$$C(r)=\lim_{N\to\infty} 1/N^2\{number\ of\ pairs\ of\ points\ with\ separation<r\}, \quad (1)$$

which is the probability that two randomly chosen points on the attractor are separated by a distance less than r; then *CD* is given by:

$$CD=\lim_{r\to 0}\frac{d\log C(r)}{d\log r} \quad (2)$$

According to [2] for data series comprising N points, the embedding dimension ($ED_{\max}$) that still provides reliable correlation dimension is:

$$ED_{\max}=2\log_{10}N \quad (3)$$

where by embedding dimension the scale of the system observation might be understood analogously to the case of visual observation of real bodies with a variable objective microscope.

The Hurst exponent test provides a numerical estimate of the predictability of a time series. It defines the relative tendency of a time series to either regress to a longer term mean value or 'cluster' in a direction – and is directly related to the fractal dimension. The Hurst exponent, H, can be estimated [5] by:

$$H=\frac{\log(R/S)}{\log T} \quad (4)$$

where T is the duration of the sample data and R/S the corresponding value of the rescaled range. The rescaled range is the measure characterizing the divergence of time series defined as the range of the mean-centered values (R) for a given duration (T) divided by the standard deviation (S) for that duration.

The values of the Hurst exponent range between 0 and 1. A Hurst exponent value close to 0.5 indicates a random signal (a Brownian time series), i.e. there is a 50% probability that future values will either increase or diminish since there is no correlation between any element and a future one. Series of this type are hard to predict.

A Hurst exponent value H between 0.5 and 1 indicates "persistent behavior", that is the time series is trending. If there is an increase from time step $[t-1]$ to $[t]$ there will probably be also an increase from $[t]$ to $[t+1]$. The same is true for decreases the larger the H value, the stronger the persistence trend. A value of H between 0 and 0.5 exists for time series with "anti-persistent behavior" – a decrease (or increase) tendency being followed by an increase (or decrease). Persistent dynamical trends are easier to predict than series falling in the other two categories.

Lyapunov exponent measures the system predictability by its sensitivity to initial conditions. It gives another insight of complex system behavior (in order to accomplish the dynamics diagnosis) characterizing highly complex systems by means of the divergence of close trajectories traced out during system evolutions in the phase space. So, Lyapunov exponent tells us the rate of divergence of nearby trajectories [14] – a key component of chaotic dynamics. There are many algorithms for calculating the largest Lyapunov exponent, but the most robust approach was introduced by Rosenstein [11] for analyzing biomedical or biological datasets, which are inherently noisy and usually short relative to the lengths required to yield adequately reliable results from this algorithm.

The basic idea of this approach is that the maximum Lyapunov exponent (λ_1) for a dynamical system can be defined from:

$$d(t)=d_0 e^{\lambda_1 t} \quad (5)$$

where $d(t)$ is the mean Euclidean distance between neighboring trajectories in state space after some evolution time t and d_0 is the initial separation (or perturbation) between neighboring starting points [11].

It is widely accepted that none of these tests could give by itself the answer to the question regarding the dynamical trend of a complex system so that at least several consecutive such analyses are needed in order to characterize the degree of complexity of system behavior and this way the dominant dynamical component. In the results section, the above mentioned computational approach was applied to the raw data signal in parallel to the corresponding smoothed data series – the numerical smoothing meaning the replacement of every data point with the average value between that data and its two close neighbors.

RESULTS AND DISCUSSION

The next figures describe the results obtained following the application of the analysis strategy mentioned above to the eye movement records. In Fig. 1 the raw and smoothed data corresponding to the $X(t)$ data series can be seen. The positive values correspond to eye shift toward the right side while the negative ones to left side eye saccadic movement.

The saccadic amplitudes were assumed to be no larger than 12 degrees since this is the maximum amplitude of the target shift. Sudden and very rapid variations having however significantly higher amplitudes (up to 25 degrees) could be recorded when the subject has blinked involuntarily; these fluctuations were diminished after smoothing the data (Fig. 1, right).

Asymmetric probability distribution was evidenced for the raw data (Fig. 2, black) because of the small probability peaks of high negative values corresponding to involuntary eye blinking that occurred accidentally during the left side saccades.

For the probability distribution test, the whole interval of the angular shifts was divided in 22 equal subintervals of two degrees width (the 12 subintervals from −12 to +12 degrees corresponding to the planned displacements of the target plus the 10 subintervals covering the extreme eye movements, i.e. the blinking leading up to 25 degree shifts during recording experiment).

The smoothing procedure has obviously eliminated part of signal fluctuations, as it can be seen in the detail of Fig. 2 where high negative amplitude bars vanished.

Power spectrum test revealed that for the raw signal (Fig. 3, left) the logarithm of square amplitude, $\log(P)$, monotonically decreases for small and medium frequency domains, suggesting the presence of high complexity dynamics (deterministic chaotic behavior); the broad graph with few peaks in the high frequency domain seems to correspond to the quasi-periodical dynamical component overlapped onto the chaotic one.

After signal smoothing, the evidence of chaotic dynamical pattern appears extended toward higher frequency domain where the large peaks vanished being replaced by the monotone slower decrease (Fig. 3, right).

Phase-space portrait test application generated the plots from Fig. 4. For raw data certain high amplitude fluctuations of the angular shift shaped large concentrically disposed polygons that are very much attenuated for the smoothed data (Fig. 4, right). In this situation the strange attractor appears more clearly in the shape of a two asymmetrical lobe object, so one can say that this test reveals the same complex dynamical components in both the recorded signal and the smoothed one; exception is related to the noise like behavioral trend that underlines the large "overall" contours from the negative half-space of the graph (corresponding to left side saccades). The *CD* values that increased over 4, corresponding to embedding dimension (*ED*) of 9 to 10, may be due to the significant random component of raw data series (Fig. 5, black). This could result from unavoidable recording noise or, as well, from the intrinsic fluctuations caused by frequent, large involuntary blinks of the subject during saccadic movement – and it is most difficult to discriminate between these two causes.

Correlation dimension (*CD*) test allowed numerical evaluation of the strange attractor fractal dimension (Fig. 5) for 1 to 10 embedding dimension (*ED*).

In the smoothed data series, as expected, the fluctuations related to electronic noise or/and to the subject blinking reflex being much diminished, in the graph *CD*(*ED*) the saturation trend resulted (Fig. 5, gray) beginning with *ED* equal to seven; this is concordant with the fact that *ED* equal to eight is given by relation (2) as highest reliable value for *CD* calculation (since the size of the data series is $N = 10^4$ so that $\log_{10}(10^4) = 4$ and $ED = 8$).

The Hurst exponent exhibits rather high values for both raw and smoothed data (Fig. 6) as can be seen from the alignment parallel to the first bisectrix of the two graphs. It indicates rather persistent behavior, which seems to be the hallmark of predictable sequences ubiquitous all over the saccadic eye movement recording duration.

Lyapunov exponent test allowed the estimation of divergence of close trajectories described by the investigated (visual-motor) system in the phase-space. Small positive values were obtained for both raw and smoothed data with considerable reduction of computing errors following smoothing procedure application.

Supplementary visualization of the Lyapunov exponent (*LE*) dependence on the embedding dimension (*ED*) is provided in Fig. 7 where the monotone decrease of *LE* value can be seen up to the *ED* equal to 4. The small positive *LE* values the system reached for *ED* higher than 4 suggest the system evolution near a bifurcation point, meaning the possible evolution toward any of two quasi-stable states that equally attract the studied system – so two possible trajectories may evolve from the bifurcation point, each leading toward another equilibrium state. Roughly, in the case of the excitable cell behavior, the general issue of bifurcated trajectories could be associated with the hypothesis of two resting potential levels co-existing with almost equal probabilities. Following each new voluntary saccade preparation and triggering, the electrical potential from the neural cell membranes could return to the initial resting potential – corresponding to the initial state at the experimental test beginning, when the subject was completely relaxed, or, another resting potential could characterize the neural membrane dynamics during the saccade recording. This way the two resting potential values could define the voluntary saccade development in the condition of the described experiment – and the Lyapunov exponent quasi-null values give the signature for distinct chaotic dynamics of the visual-motor system. Our further research task will be focused on the identification of the specific neural areas responsible for such chaotic behavior, based on the below considerations.

One of the major functions of the central nervous system is the generation of movement in response to sensory stimulation [1]. The visual guidance of saccadic eye movement represents one form of sensory-to-motor transformation that has contributed significantly to the understanding of motor control of saccadic eye movements. From the biophysical viewpoint the key segment of the neural pathway that is mainly responsible for complex chaotic dynamics would be characterized by voltage gated potassium channels that could impede the recovery of the initial resting potential possibly due to their sensitivity diminution during repeated saccadic activation. So, the membrane re-polarization could occur only partially for some saccades while for others it could be complete – which may explain the system oscillation between two stable states, as suggested by near-zero positive Lyapunov exponent.

CONCLUSIONS

Following the application of the computational tests based on chaos theory to the analysis of saccadic eye movements in the frame of a specific experimental design, a chaotic dynamical trend was found. Possible alternation in the functioning of some neural cell potassium channels due to repeated voluntary saccades could underlie the observed results.

Acknowledgements

This research was supported by FP7 PEOPLE 2010 IRSES CERVISO project.

REFERENCES

1. Catz N, Thier P. Neural control of saccadic eye movements. Dev. Ophthalmol. 2007; 40:52–75. [PubMed: 17314479]
2. Eckmann JP, Ruelle D. Fundamental limitations for estimating dimensions and Lyapunov exponents in dynamical systems. Physica D. 1992; 56:185–187.
3. Fell J, Mann K, Röschke J, Gopinathan MS. Nonlinear analysis of continuous ECG during sleep. I. Reconstruction. Biol. Cybern. 2000; 82:477–483. [PubMed: 10879431]
4. Grassberger P, Procaccia I. Characterization of strange attractors. Phys. Rev. Lett. 1983; 50:346–349.
5. Kale M, Butar FB. Fractal analysis of time series and distribution. Properties of Hurst exponent. J. Math. Sci. Math. Ed. 2011; 5:8–19.
6. Kandel, ER.; Schwartz, JH.; Jessell, TM. Principles of Neuroscience. New York: McGraw-Hill; 2000.
7. Kannathal N, Acharya UR, Alias F, Tiboleng T, Puthusserypady SK. Nonlinear analysis of EEG signals at different mental states. Biomed. Eng. OnLine. 2004; 3:7. [PubMed: 15023233]
8. Lai YC, Osorio I, Harrison MA, Frei MG. Correlation-dimension and autocorrelation fluctuations in epileptic seizure dynamics. Phys. Rev. E. 2002; 65:031921.
9. Lamberts J, Van den Broek PLC, Bener L, Van Egmond J, Dirksen R, Coenen AML. Correlation dimension of the human electroencephalogram corresponds with cognitive load. Neuropsychobiology. 2000; 41:149–153. [PubMed: 10754429]
10. Owis MI, Abou-Zied AH, Abou-Bakr MY, Kadah YM. Study of features based on nonlinear dynamical modelling in ECG arrhythmia detection and classification. IEEE Trans. Biomed. Eng. 2002; 49:733–736. [PubMed: 12083309]
11. Rosenstein MT, Collins JJ, Deluca CJ. A practical method for calculating largest Lyapunov exponents from small data sets. Physica D. 1993; 65:117–134.
12. Schmeisser ET, Mcdonough JM, Bond M, Hislop PD, Epstein AD. Fractal analysis of eye movements during reading. Optom. Vis. Sci. 2001; 78:805–814. [PubMed: 11763254]
13. Shelhamer M. Correlation dimension of optokinetic nystagmus as evidence of chaos in the oculomotor system. IEEE Trans. Biomed. Eng. 1992; 39:1319–1321. [PubMed: 1487297]

14. Shelhamer M. Nonlinear dynamic systems evaluation of `rhythmic' eye movements (Optokinetic Nystagmus). J. Neurosci. Meth. 1998; 83:45–56.
15. Sprott, JC.; Rowlands, G. Chaos Data Analyzer. New York: American Institute of Physics; 1995.
16. Takens, F., et al. Detecting strange attractor in turbulence. In: Rand, DA.; Young, LS., editors. Dynamical Systems of Turbulence. Vol. 898. Berlin: Springer-Verlag; 1981. p. 366-381.

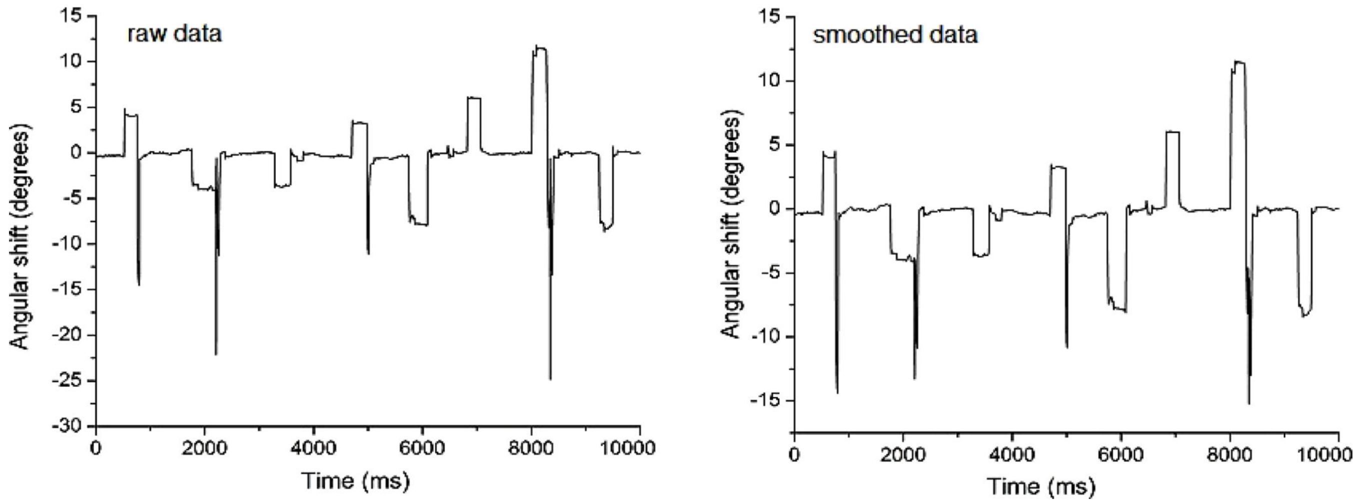

Fig. 1.
The dynamics of angular shift $X(t)$ during saccadic eye movement for raw and smoothed data.

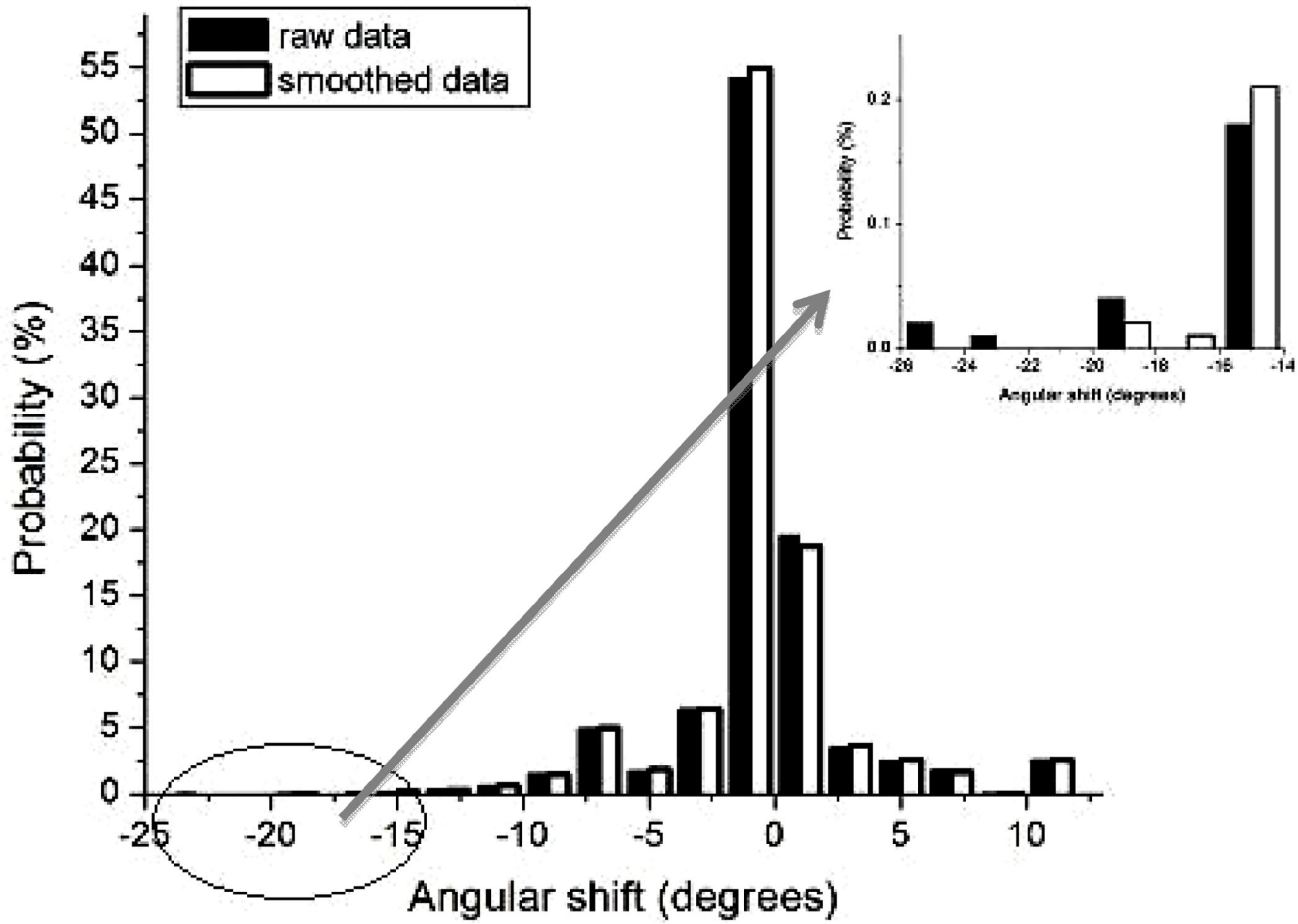

Fig. 2.
Probability distribution histograms for saccadic eye movements: black – raw data; gray – three times smoothed data; (up-right: detail for asymmetric negative value interval).

NIH-PA Author Manuscript

NIH-PA Author Manuscript

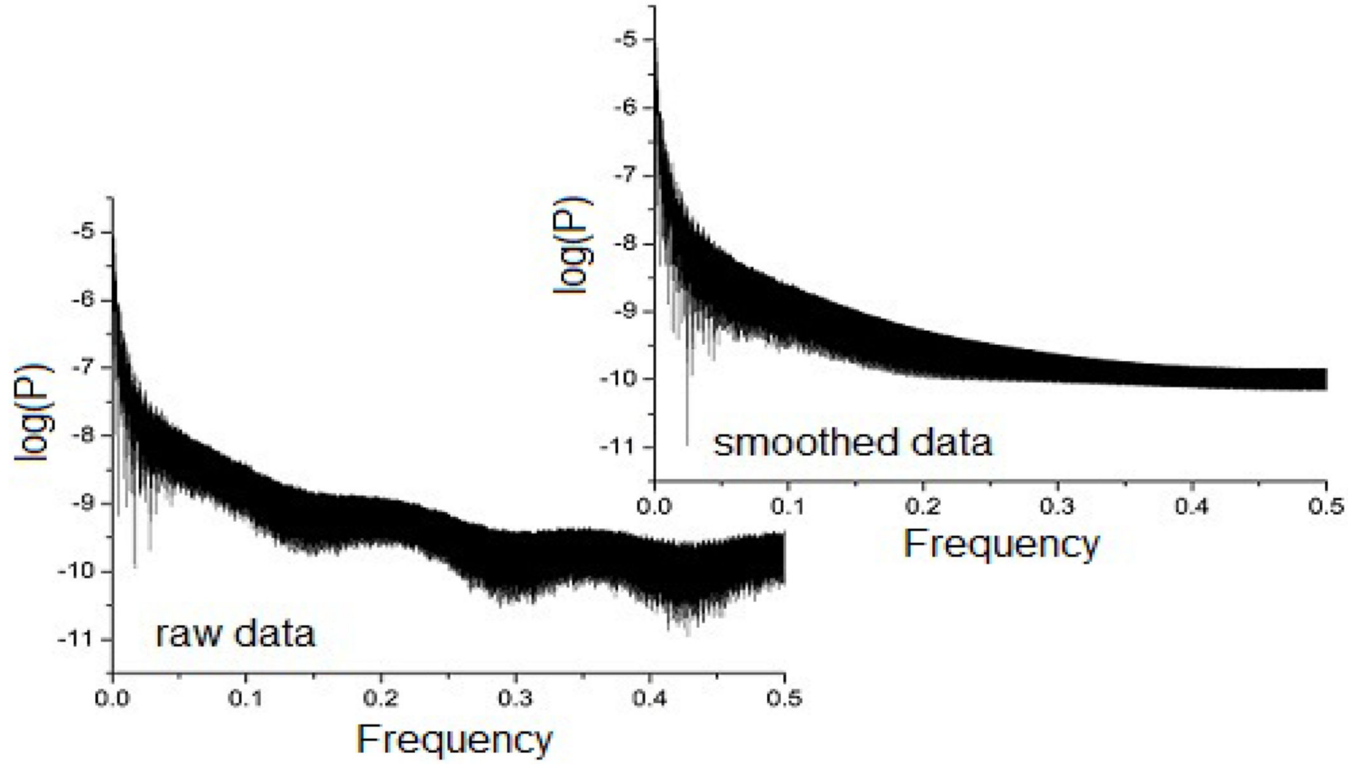

Fig. 3.

Linear logarithmic representation of the power spectrum generated by fast Fourier transformation of raw and smoothed data.

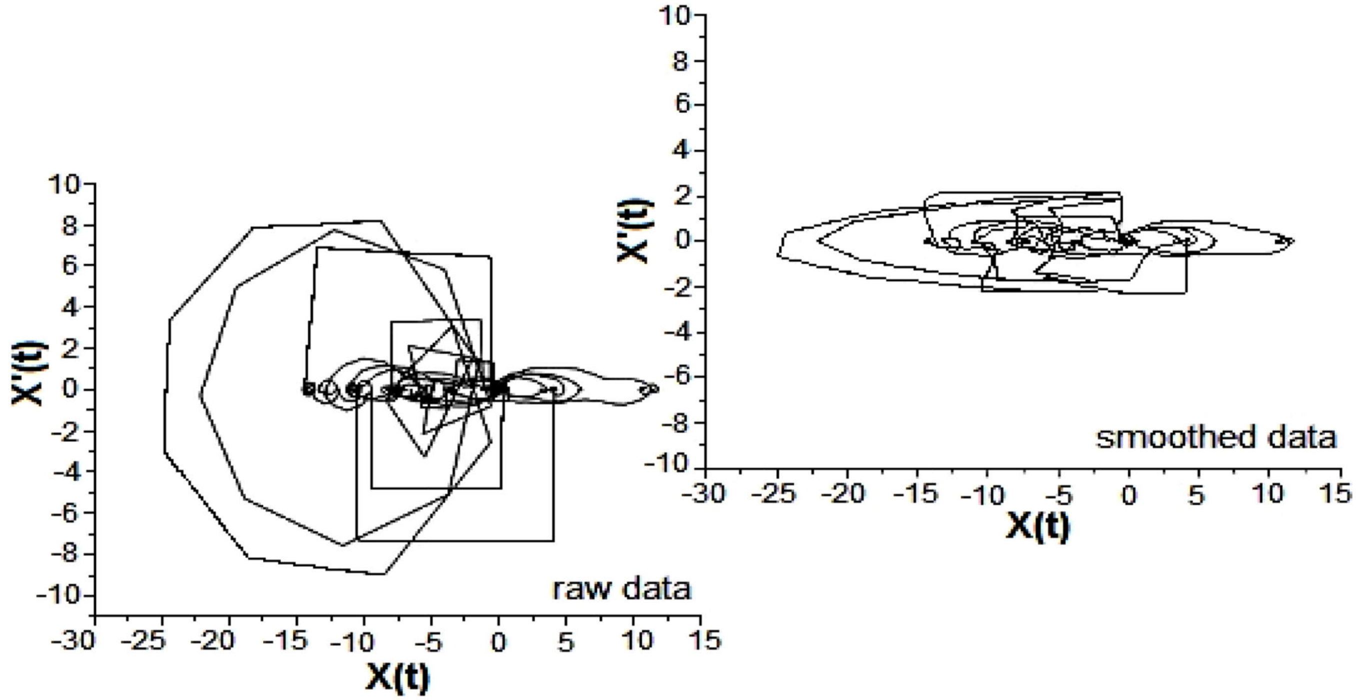

Fig. 4.

The phase space portrait ($X(t)$ vs. $X'(t)$) for raw and smoothed data; $X(t)$ is the angular recorded shift while $X'(t)$ is its derivative.

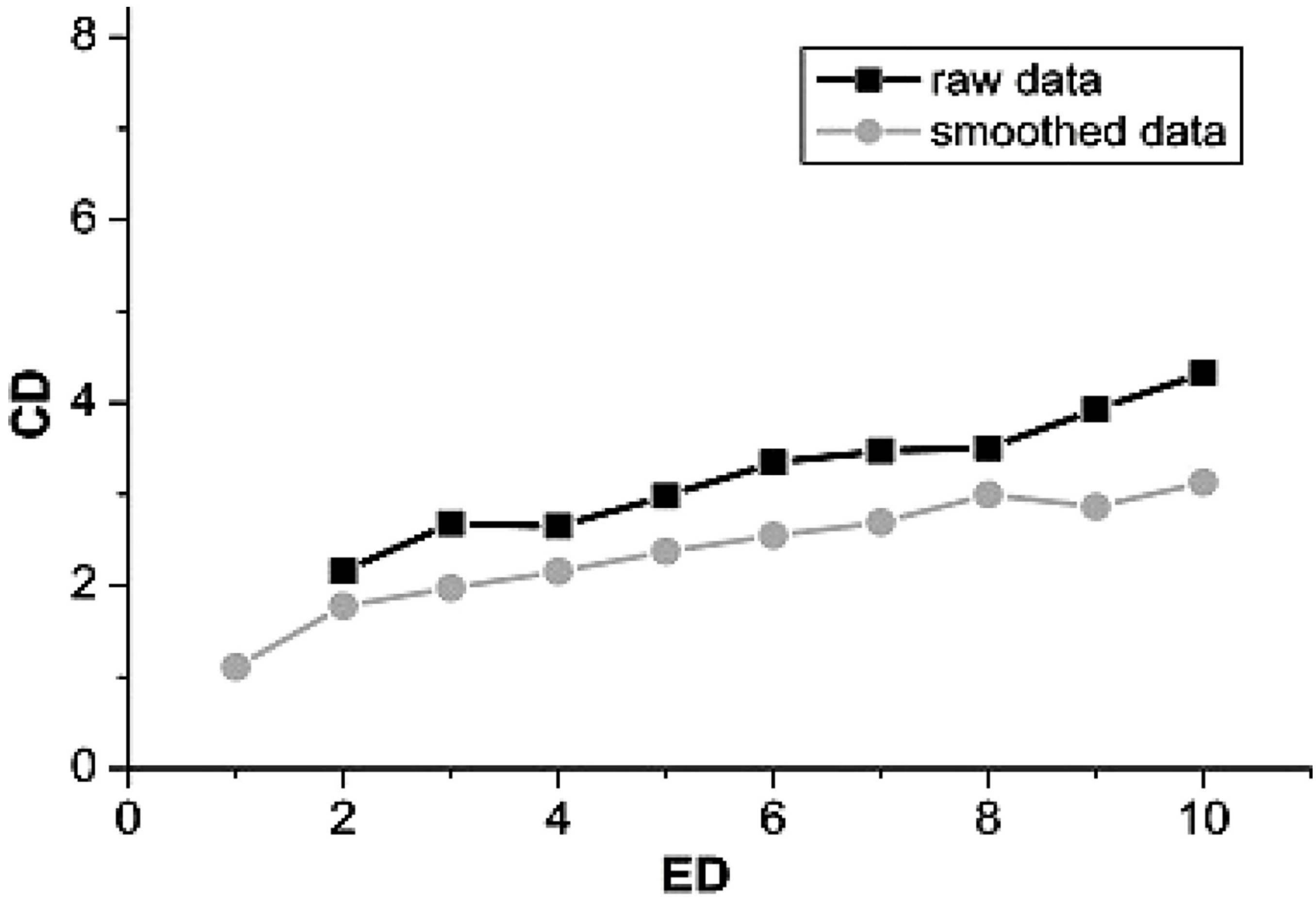

Fig. 5.
The correlation dimension (*CD*) *versus* embedding dimension (*ED*) for raw (black graph) and smoothed data (gray graph) (time delay $n = 1$).

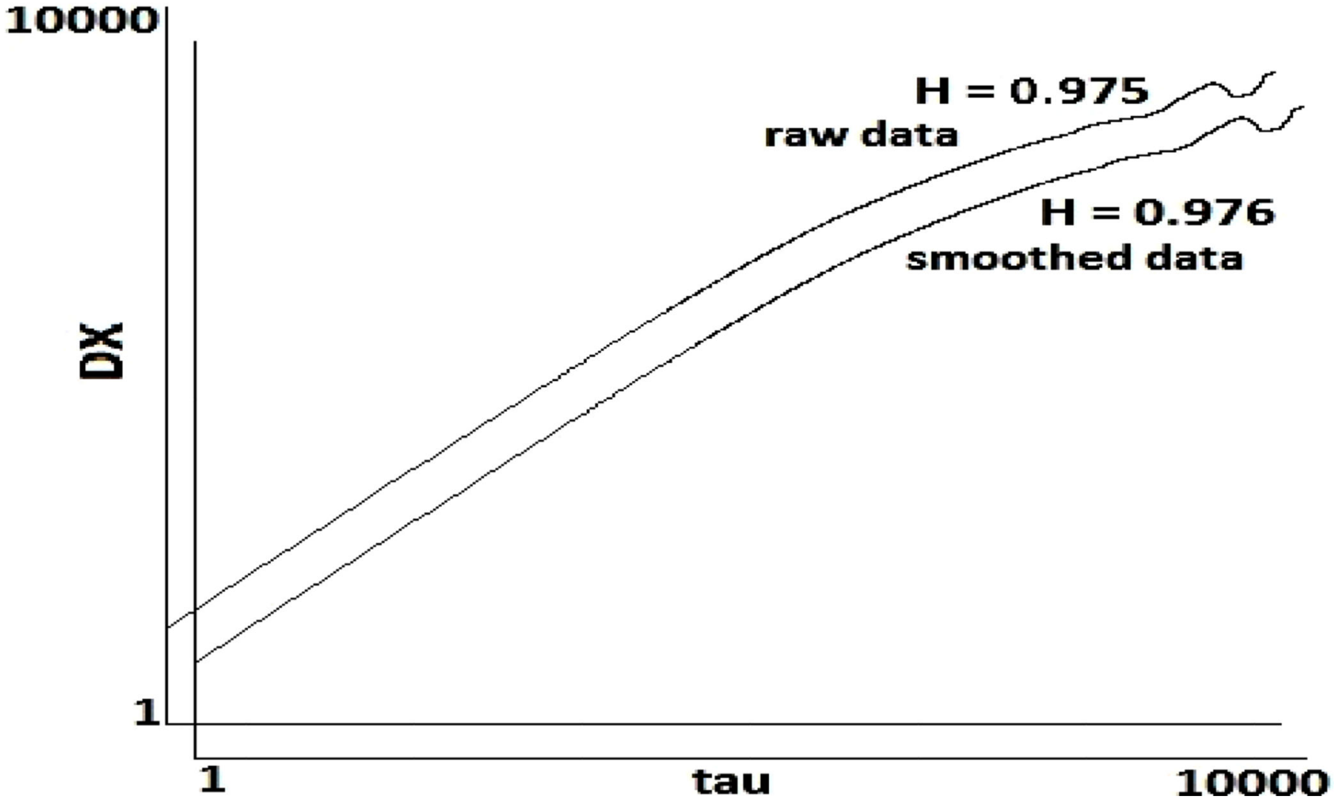

Fig. 6.

Hurst exponent for raw data and smoothed data; *DX* – the angular shift displacement (variation) for every time value within the data series.

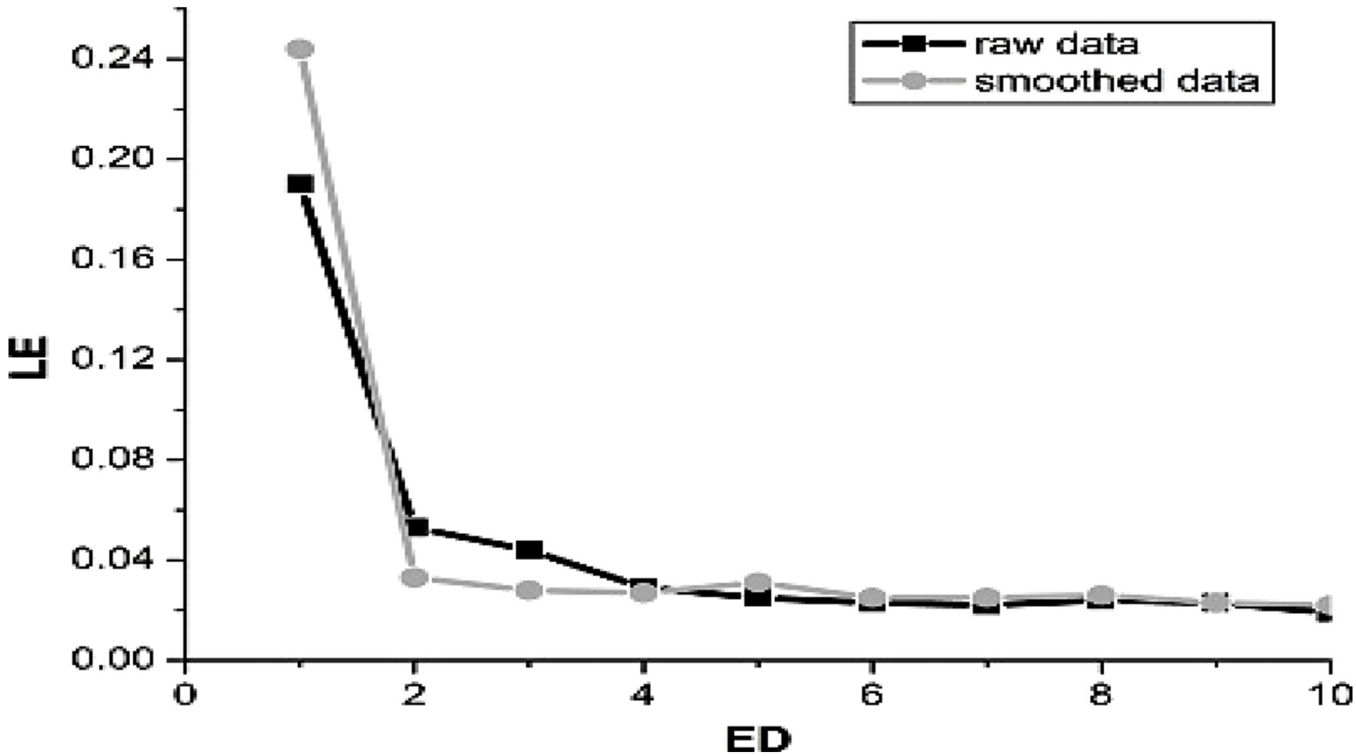

Fig. 7.
The Lyapunov exponent (*LE*) *versus* embedding dimension (*ED*) for raw data and three times smoothed data.